Journal of Catalysis 266 (2009) iii–ix

Contents lists available at ScienceDirect

Journal of Catalysis

journal homepage: www.elsevier.com/locate/jcat

Journal of Catalysis Vol. 266, Issue 2, 2009

Contents

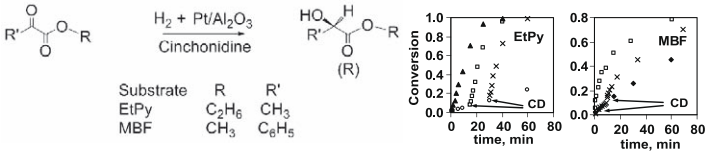

Upon hydrogenation of activated ketones the injection of cinchonidine (CD) results in immediate conversion increase, consequently the rate enhancement has to be an intrinsic property of the system.

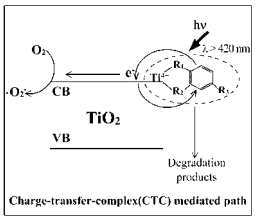

Charge transfer complexes enhance the photo catalytic activity of titania for degradation of organic pollutants under visible light.

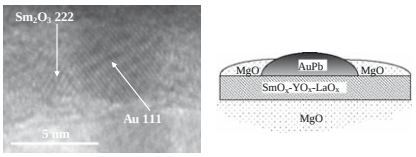

MgO-supported gold catalysts modified by V, Pb, Sm, La and Y have been investigated in order to elucidate the role of modifiers in preferential CO oxidation. Synergistic effect of different components on the catalytic performance has been observed which is due to alloying of gold with Pb and modification of the nanoenvironment of gold by metal oxides.

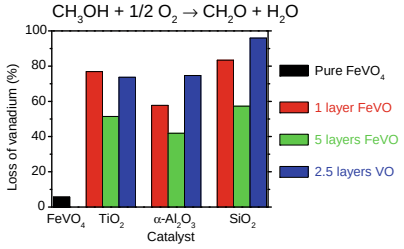

A considerable loss of the vanadium supported on TiO_2, α-Al_2O_3 and SiO_2 is observed after 5 days of operation in methanol oxidation with 10% methanol and 10% O_2 at 300 °C and at differential conditions.

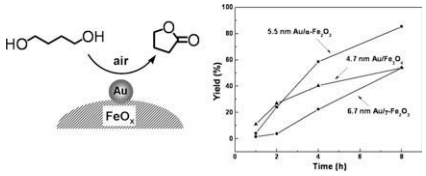

Gold supported on different iron oxides shows different catalytic behavior in the oxidation of 1,4-butanediol to γ-butyrolactone. The support effect is more significant than the gold particle size effect.

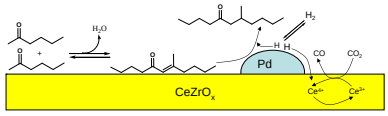

The primary pathway for aldol condensation/hydrogenation of 2-hexanone on Pd/$CeZrO_x$ yields 7-methyl-5-undecanone. Inhibiting effects of CO_2 are ameliorated by the presence of Ce^{3+}, formed by H_2 spillover from Pd and leading to reduction of CO_2 to CO.

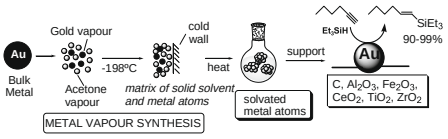

Supported (C, Al_2O_3, Fe_2O_3, CeO_2, TiO_2 and ZrO_2) gold nanoparticles were easily prepared starting from gold/acetone solutions generated according to the Metal Vapour Synthesis technique. The catalytic activity of Au nanoclusters was tested in the hydrosilylation of 1-hexyne, and it resulted influenced by two major factors: particle size and support selection.

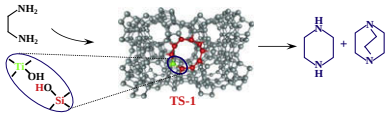

The internal silanols of TS-1 are active and selective for the intermolecular condensation of ethylenediamine to piperazine and triethylenediamine.

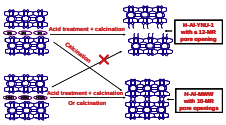

H-Al-YNU-1 with a 12-MR pore opening and H-Al-MWW with different Si/Al ratios were postsynthesized in the presence of piperidine (PI) and hexamethyleneimine (HMI) with the ion-exchange of Na^+ with NH_4^+ unnecessary. H-Al-YNU-1 was not obtained by acid treating and subsequently calcining the Al-MWW lamellar precursor synthesized with HMI, but it could be prepared in such a way when PI was used, and showed high activity in alkylation of anisole with $C_6H_5CH_2OH$ and acylation of anisole with $(CH_3CO)_2O$.

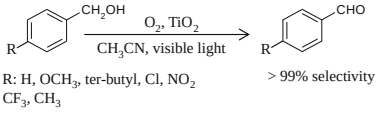

Highly efficient selective photocatalytic oxidation of benzyl alcohol and its derivatives into benzaldehydes has been realized on TiO_2 under visible light irradiation.

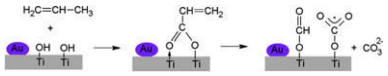

An additional route to deactivation of Au/TiO_2 in the oxidation of propene is proposed.

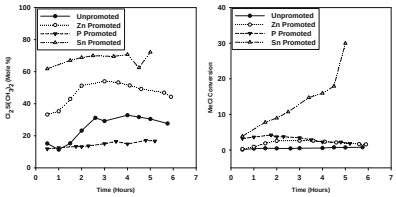

The Direct Synthesis, or Rochow Synthesis, produces methylchlorosilanes through the reaction of methyl chloride (MeCl) with a contact mass composed of Si and Cu (catalyst), which is promoted with part-per-million amounts of Zn, Sn, and P. Attenuated total reflection infrared spectroscopy was used to probe the surface composition of the contact mass *in situ* as a function of promoter and these results were correlated to product distributions that were determined by flow reactor studies. One significant correlation was that the presence of Sn led to an enhancement in CH_3 surface concentration, MeCl conversion, and selectivity toward dimethyldichlorosilane product relative to unpromoted contact masses and contact masses promoted with zinc; it was noted that P-promoted surfaces also enhance surface CH_3 concentration, but did not exhibit the increase in MeCl conversion and selectivity toward dimethyldichlorosilane.

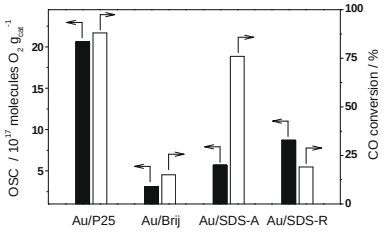

The reversible uptake and reactive removal of active oxygen, and its relation to the CO oxidation activity were investigated on different mesoporous Au/TiO_2 catalysts and on a non-porous Au/TiO_2 catalyst. Variation of the support has a distinct influence on the ability to store active oxygen and its relation to the activity.

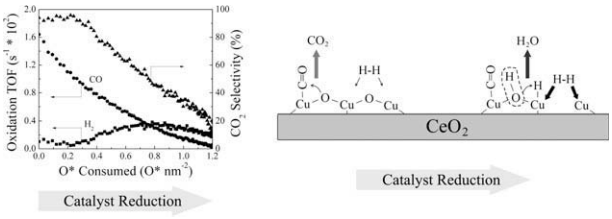

Reaction mechanisms and active sites are studied for CO and H_2 oxidation on CuO_x–CeO_2 catalysts. High selectivity results primarily from an inhibition of H_2 dissociation by oxidized sites.

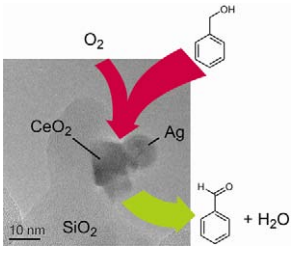

A physical mixture of Ag–SiO_2 and CeO_2 nanoparticles catalyzes the selective oxidation of alcohols to the corresponding aldehydes in an efficient way.

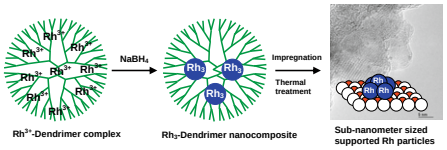

Nearly uniform Rh particles with sizes below 1 nm were prepared on a ZrO_2 support via a dendrimer-mediated synthetic route. The coordination environment of Rh was monitored by EXAFS during all preparation steps and HRTEM was used to image the resulting supported Rh nanoparticles. The structure-sensitive ethane hydrogenolysis reaction was used to probe the catalytic properties of the Rh/ZrO_2 materials produced.

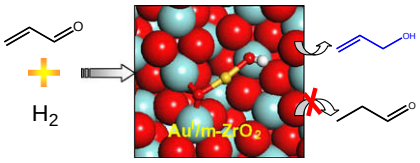

First principle calculations show that single Au cations present at ZrO_2 stepped sites at room temperatures can selectively hydrogenate acrolein to allyl alcohol.

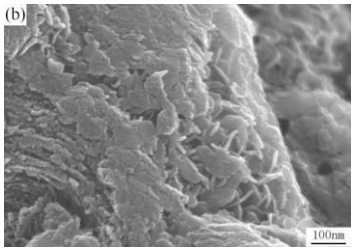

A Ni^{2+}—Al^{3+}—CO_3^{2-}-layered double hydroxide precursor has been synthesized in the pores of spherical γ-Al_2O_3 particles. After calcination and reduction, a highly dispersed Ni/γ-Al_2O_3 catalyst was obtained.

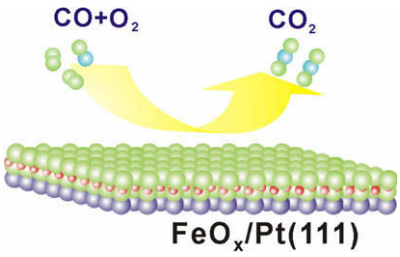

Ultrathin FeO(1 1 1) films grown on Pt(1 1 1) unexpectedly showed high activity towards CO oxidation. The reaction proceeds through the formation of a well-ordered, oxygen-rich FeO_x ($1 < x < 2$) film. In CO-rich ambient the film dewets the Pt surface, ultimately resulting in highly dispersed iron oxide particles on Pt(1 1 1).

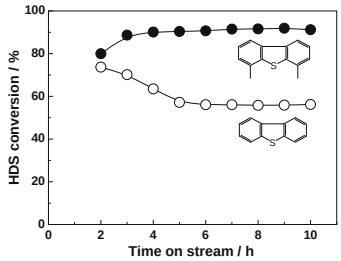

A sulfidation–reduction procedure was used to prepare a MoP/MCM-41 catalyst, which showed considerably a higher hydrodesulfurization (HDS) activity, especially for 4,6-dimethyldibenzothiophene, than the counterpart prepared by conventional method.

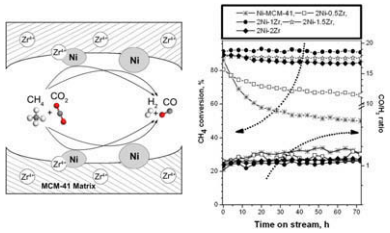

Ni–Zr–MCM-41 catalysts exhibited remarkably enhanced catalytic activity and long-term stability due to the anchoring effect of Zr^{4+} and partial activation of CO_2 by Zr^{4+}.

LETTER TO THE EDITOR

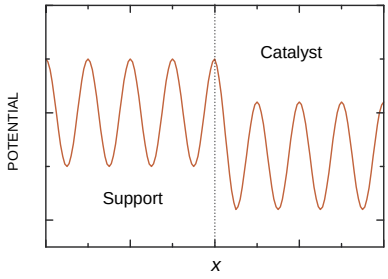

Schematic potential energy for adsorbate diffusion along the surface.

RESPONSE TO LETTER TO THE EDITOR